Low-temperature spin-glass behavior in a diluted dipolar Ising system

Juan J. Alonso

Física Aplicada I, Universidad de Málaga, 29071 Málaga, Spain
and Instituto Carlos I de Física Teórica y Computacional, Universidad de Granada, 18071 Granada, Spain

Using Monte Carlo simulations, we study the character of the spin-glass (SG) state of a site-diluted dipolar Ising model. We consider systems of dipoles randomly placed on a fraction x of all L^3 sites of a simple cubic lattice that point up or down along a given crystalline axis. For $x \lesssim 0.65$ these systems are known to exhibit an equilibrium spin-glass phase below a temperature $T_{sg} \propto x$. At high dilution and very low temperatures, well deep in the SG phase, we find spiky distributions of the overlap parameter q that are strongly sample dependent. We focus on spikes associated with large excitations. From cumulative distributions of q and a pair correlation function averaged over several thousands of samples we find that, for the system sizes studied, the average width of spikes, and the fraction of samples with spikes higher than a certain threshold, does not vary appreciably with L. This is compared with the behavior found for the Sherrington-Kirkpatrick model.

I. INTRODUCTION

Complex systems are present in life and social sciences, information systems, and economics [1]. In these systems, different random distributions of their microscopic constituent parts give rise to diverse values of some macroscopic properties [2]. A paradigmatic model in statistical physics that exhibits complexity is the Sherrington-Kirkpatrick (SK) model [3], where the couplings between any pair of spins is randomly fixed to be ferromagnetic (FM) or antiferromagnetic (AF) regardless of the spin-spin distance. This model has both quenched spatial-disorder and frustration [4], the two essential ingredients of spin glasses (SG) [5,6]. Its exact solution [7] shows the existence of replica symmetry breaking (RSB) [8]: Different identical replicas of a sample $\mathcal{J}$ with the same couplings may, in the thermodynamic limit, stay trapped in different states within the set of infinitely many pure states. These pure states are diverse in the sense that they are sample dependent. The distribution of the overlap q between states of a given sample, $p_{\mathcal{J}}(q)$, is found to be a comblike superposition of infinitely many δ-like spikes. In the macroscopic limit, after averaging over spatial disorder, the overlap distribution is given by $p(q) = \delta(q - q_m) + f(q)$, where $f(q)$ is a nonzero smooth function for $q < q_m$ and zero otherwise.

Whether the RSB picture describes correctly the behavior of *realistic* spin glasses, such as dilute metallic alloys or concentrated insulators [9], is still a matter of debate. The three-dimensional (3D) Edwards-Anderson model (EA) [10], in which only nearest-neighbor spins interact, is the simplest one with the essential ingredients of short-ranged SGs. No exact solution exists for the EA model, but there is consensus on the existence of a SG phase based on numerical simulations [11]. The applicability of a RSB scenario to the SG phase of the EA model is still controversial [12]. In the so-called *droplet picture*, the SG phase is described in terms of a unique state (paired with the one obtained by a global spin inversion) with excitations that are compact droplets of the inverted state [13]. According to this scenario, $p_{\mathcal{J}}(q)$ distributions do not exhibit diversity—in the sense that $p_{\mathcal{J}}(q)$ is independent of $\mathcal{J}$—and the averaged $p(q)$ becomes a single δ function $\delta(q - q_m)$: $p(q)$ is said to be *trivial*. Some *trivial-nontrivial*

scenarios, between the droplet and RSB pictures, have also been proposed [14]. Early MC simulations point to a *nontrivial* scenario [15], but it has been found that the asymptotic behavior for $p(q \simeq 0)$ is only reached at very large sizes even for toy droplet models [16].

There is growing interest in the study of sample-to-sample fluctuations of $p_{\mathcal{J}}(q)$ from their average $p(q)$ [17]. Some recently proposed quantities give information on the height [18] and average width [19] of spikes found in $p_{\mathcal{J}}(q)$. By MC simulations, these quantities have been found to be nearly size-independent for the EA model, in contradiction with RSB predictions. However, these results have been criticized to be far away from the asymptotic regime [20,21]. Some have found more useful to study the statistics of the area under $p_{\mathcal{J}}(q)$ for $q < q_m$ [17,20]. The numerical study of SG models distinct from the SK and EA models has shed some light on the virtues and weaknesses of these new probes for measuring diversity [22,23].

Frustration in the SK and EA models comes from the competition between randomly distributed FM and AF couplings. However, frustration may also appear in fully occupied systems with no quenched disorder, such as the Ising model with pure AF interactions on a FCC lattice [24]. Dipoles packed in crystalline arrangements have frustration, exhibiting magnetic order that is strongly dependent on the lattice structure [25,26]. Some ferroelectrics [27] and magnetic insulators such as LiHoF$_4$ are known to be well described by arrays of parallel Ising dipoles that behave as uniaxial ferromagnets [28]. In dipolar Ising systems (DIS), dilution put together with the built in *geometric frustration* results in SG behavior [29]. LiHo$_x$Y$_{1-x}$F$_4$ is one example that has been extensively studied. Experiments [30] have found a SG phase for concentration $x = 0.16$ and a FM phase for $x > x_c$ where $x_c \simeq 0.25$. Recent MC simulations of systems of classical Ising dipoles placed on a fraction x of the sites of the LiHoF$_4$ tetragonal lattice have found a SG phase for all $0 < x \lesssim 0.25$ for temperatures below a SG transition temperature $T_{sg} \propto x$ [31,32].

Here we study a site-diluted system of L^3 dipoles, which are placed at random on a fraction x of the sites of a simple cubic

(SC) lattice and point up or down along one of the principal axis. In the limit of low concentrations details of the lattice are expected to become irrelevant. Therefore, our model at low concentrations has direct connection with the experimental and numerical work mentioned above. In previous MC work [33] we have calculated the entire diagram of the system and found a SG phase for $0 < x < x_c$, where $x_c \simeq 0.65$ with the SG transition temperature given by $T_{sg}(x) \simeq x$. We found from the following evidence that the SG phase behaves marginally: (i) the mean values $q_1 = \langle |q| \rangle$ decrease algebraically with L; (ii) averaged overlap distributions of q/q_1 appear wide and independent of L; (iii) ξ_L/L, where ξ_L is a correlation length [34], rises with L at constant T but extrapolates to finite values as $1/L \to 0$. All of this is consistent with quasi-long-range order in the SG phase, Neither the droplet model nor a RSB scenario fit with this marginal behavior.

The main aim of this paper is to study whether diversity may emerge in this *geometrically frustrated* model at low temperatures and high dilution, rather deep in its marginal SG phase by using the probes for measuring diversity, in the sense that was specified above. The paper is organized as follows. In Sec. II we define the model, give details on the parallel tempered Monte Carlo (TMC) algorithm [35], and define the quantities we compute. We present results in Sec. III, followed by concluding remarks in Sec. IV.

II. MODEL, METHOD, AND MEASURED QUANTITIES

A. Models

We consider site-diluted systems of classical Ising spins on a SC lattice. All spins are parallel and point along the z axis of the lattice. At each lattice site a spin is placed with probability x. These spins are coupled solely by dipolar interactions. The Hamiltonian is given by

$$\mathcal{H} = \sum_{\langle i,j \rangle} T_{ij} \sigma_i \sigma_j, \tag{1}$$

where the summation runs over all pairs of occupied sites i and j except $i = j$, $\sigma_i = \pm 1$ on any occupied site i,

$$T_{ij} = \varepsilon_a (a/r_{ij})^3 \big(1 - 3z_{ij}^2/r_{ij}^2\big), \tag{2}$$

where r_{ij} is the distance between i and j sites, z_{ij} is the z component of r_{ij}, ε_a is an energy, and a is the SC lattice constant. In the following, temperatures shall be given in terms of ε_a/k_B.

Note that T_{ij} values are not distributed at random but depend only on the orientation of vectors $\mathbf{r}_{ij}$ on a SC lattice. This is why DIS exhibit AF order at concentrations $x > x_c$ [26,33]. This is to be contrasted with *random-axes* dipolar models [36], in which Ising spins point along directions that are chosen at random, introducing randomness on bond strengths.

In this paper we study DIS with $x << x_c$ for which the details of the lattice structure are not important. Not surprisingly, in the limit of high dilution the behavior of DIS and the LiHo$_x$Y$_{4-x}$F$_4$ system (a well-known dipolar ferromagnet for $x = 1$) have been found to be closely related [32,33].

For comparison, we study also the SK model: a set of $N = L^3$ Ising spins $\sigma_i = \pm 1$ with interaction energies between

TABLE I. Simulation parameters for the SK model. The number of spins is $N = L^3$, T_{min} (T_{max}) is the lowest (highest) temperature and Δ is the temperature step in our TMC simulations. The number of MC sweeps for equilibration is t_0. Measurements are taken in the time interval $[t_0, 2t_0]$. The number of samples with different realizations of (quenched) disorder is N_s.

L	T_{min}	T_{max}	Δ	t_0	N_s
4	0.16	1.60	0.04	10^5	10^5
6	0.16	1.60	0.04	10^5	1.4×10^5
8	0.16	1.60	0.04	2×10^5	10^5

any pair of spins at sites i and j given by $J_{ij}\sigma_i\sigma_j$ with $J_{ij} = \pm 1/\sqrt{N}$ chosen randomly, without bias, for all ij site pairs.

B. Method

For the models described in Sec. II A we have simulated a large number N_s of independent *samples*. By a *sample*, $\mathcal{J}$, we mean a system with a given quenched distribution of empty sites for DIS (a quenched distribution of random couplings J_{ij} for the SK model). The number of samples we average over is given in Tables I and II. We have tried not to make N_s smaller with increasing L. This is because statistical errors are independent of L, because of non-self-averaging. (However, for DIS with $L = 10$, we could only do 1.2×10^4 samples. That took an Intel 8-core Xeon processor E5-2670 some 60 years' worth of CPU time.)

Thermal averages come from averaging over the time range $[t_0, 2t_0]$, where t_0 is the equilibration time. We further average over the N_s samples with different realizations of quenched disorder.

In order to accelerate equilibration at low temperatures in the glassy phase we use a parallel tempered Monte Carlo (TMC) algorithm [35]. We apply the TMC algorithm as follows. We run in parallel a set of n identical replicas of each sample at different temperatures in the interval $[T_{min}, T_{max}]$ with a separation Δ between neighboring temperatures. Each replica starts from a completely disordered spin configuration $\{\sigma_i\}$. We apply the TMC algorithm to any given sample in two stages. In the first stage, the n replicas of the sample $\mathcal{J}$ evolve independently for 10 MC Metropolis sweeps [37]. All dipolar fields throughout the system are updated every time a spin flip is accepted. In the second stage, we give any pair of replicas evolving at temperatures T and $T - \Delta$ a chance to exchange states between them following standard

TABLE II. Same as in Table I but for DIS with concentration $x = 0.35$. In our TMC runs for DIS we have chosen a temperature step of Δ_1 for the temperature interval $[T_{min}, T_m]$ and a bigger one, Δ_2, for $[T_m, T_{max}]$.

L	T_{min}	T_m	T_{max}	Δ_1	Δ_2	t_0	N_s
4	0.05	0.4	1.65	0.025	0.05	5×10^6	2×10^5
6	0.05	0.4	1.65	0.025	0.05	5×10^6	1.1×10^5
8	0.05	0.4	1.65	0.025	0.05	5×10^6	10^5
10	0.075	0.4	1.65	0.025	0.05	5×10^7	1.2×10^4

tempering rules which satisfy detailed balance [35]. These exchanges allow all replicas to diffuse back and forth from low to high temperatures and reduce equilibration times for the rough energy landscapes of SGs. We find it helpful to have the highest temperature $T_{\max}$ larger than $1.6 \times T_{\text{sg}}$. We choose Δ such that at least 30% of all attempted exchanges are accepted for all T.

For DIS we use periodic boundary conditions (PBC). Details of the PBC scheme we use can be found in Ref. [33]. We let a spin on an occupied site i interact only with spins within an $L \times L \times L$ cube centered on i. In spite of the long-range nature of the dipolar interaction, we do not perform Ewalds's summations and exclude any contributions from repeated copies of the lattices beyond this box. This introduces an error which was shown for DIS in SC lattices to vanish as $L \to \infty$, regardless of whether the system is in the paramagnetic, AF, or SG phase (see Appendix I in Ref. [33]). This result is not applicable to an inhomogeneous FM phase that may obtain on other lattices such as in LiHoF$_4$.

C. Measured quantities

Measurements were performed after two averagings: first, over thermalized states of a given sample and, second, over a number N_s of different samples.

Given an observable u, we let $u_{\mathcal{J}} = \langle \text{u} \rangle_T$ stand for the thermal average of sample $\mathcal{J}$ and $u = [u_{\mathcal{J}}]_{\mathcal{J}}$ for the average over samples.

We measure the Edwards-Anderson overlap parameter [10],

$$q = N^{-1} \sum_j \sigma_j^{(1)} \sigma_j^{(2)}, \tag{3}$$

where $\sigma_j^{(1)}$ and $\sigma_j^{(2)}$ are the spins on site j of identical replicas (1) and (2) of a given sample. Clearly, q is a measure of the spin configuration overlap between configurations of the two replicas.

For each sample $\mathcal{J}$ we compute the overlap probability distribution $p_{\mathcal{J}}(q)$. The mean overlap distribution $p(q)$ over all replicas is defined by

$$p(q) = [p_{\mathcal{J}}(q)]_{\mathcal{J}}. \tag{4}$$

We also measure the mean-square deviations of $p_{\mathcal{J}}(q)$, from the average $p(q)$,

$$\delta p(q)^2 = [\{p_{\mathcal{J}}(q) - p(q)\}^2]_{\mathcal{J}}. \tag{5}$$

In order to probe for RSB behavior we focus on overlaps between states that belong to different basins of attraction. With that aim, we compute the integrated probability functions defined by

$$X_{\mathcal{J}}^Q = \int_{-Q}^{Q} p_{\mathcal{J}}(q) dq, \tag{6}$$

$$\Delta_{\mathcal{J}}^Q = \left(\int_{-Q}^{Q} \{p_{\mathcal{J}}(q) - p(q)\}^2 dq \right)^{1/2}, \tag{7}$$

and calculate their corresponding averages X^Q and Δ^Q. An advantage of working with quantities integrated over the interval $q \in (-Q, Q)$ is that statistical errors come smaller.

Given that $X_{\mathcal{J}}^Q$ is a ($\mathcal{J}$-dependent) random variable, it makes sense to explore how this variable is distributed. Following Ref. [20], we define its cumulative distribution $\Pi_c^X(z)$ as the fraction of samples having $X_{\mathcal{J}}^Q < z$.

Yucesoy *et al.* [18] have proposed very recently an observable that is sensitive to spikes in the overlap distributions $p_{\mathcal{J}}(q)$ of individual samples. They consider the maximum value of $p_{\mathcal{J}}(q)$ for $q \in (-Q, Q)$,

$$\widetilde{p}_{\mathcal{J}}^Q = \max \left\{ p_{\mathcal{J}}^Q(q) : |q| < Q \right\}, \tag{8}$$

and count a sample as *peaked* if $\widetilde{p}_{\mathcal{J}}^Q$ exceed some specified value. We compute the cumulative distribution $\Pi_c^{\widetilde{p}}(z)$ of $\widetilde{p}_{\mathcal{J}}^Q$ as the fraction of samples having $\widetilde{p}_{\mathcal{J}}^Q < z$.

In previous papers [19] we have obtained additional information on the shape and width of spikes from a *pair correlation function*. Let $f_{\mathcal{J}}(q_1, q_2) \equiv p_{\mathcal{J}}(q_1) p_{\mathcal{J}}(q_2)$,

$$G_{\mathcal{J}}^Q(q) = \int_0^Q \int_0^Q dq_1 dq_2 \, \delta(q_2 - q_1 - q) f_{\mathcal{J}}(q_1, q_2), \tag{9}$$

and let $G^Q(q)$ be the average of $G_{\mathcal{J}}^Q(q)$ over samples. We compute the normalized function

$$g^Q(q) = G^Q(q) / \int_{-Q}^{Q} G^Q(q) dq, \tag{10}$$

which is the conditional probability density that $q = q_2 - q_1$, given that $q_1, q_2 \in (0, Q)$. Note that $g^Q(q)$ is largest at $q = 0$ and that $g^Q(q) = g^Q(-q)$, since $p_{\mathcal{J}}(q) = p_{\mathcal{J}}(-q)$. It makes sense to define the width of $g^Q(q)$ as

$$w^Q = 1/g^Q(0), \tag{11}$$

which is a measure of pattern thermal fluctuations for $|q| < Q$.

An additional interpretation of $g^Q(q)$ is possible for sufficiently small T ($T \lesssim 0.4 T_{\text{sg}}$, roughly) so individual spikes are clearly discernible. Assume, in addition, that Q is sufficiently small so contributions from samples with more than one spike in the $0 < q < Q$ range is negligible. Then, (i) finding on each sample one such spike, if there is one, (ii) calculating the self-overlap of such spike with a copy of itself shifted by a distance q, (iii) adding the resulting function of q over all samples, and (iv) normalizing gives $g^Q(q)$. To that extent, $g^Q(q)$ stands for an average over all spikes on the $0 < q < Q$ range. In Ref. [19] we have also shown that if the width of spikes does not vary over different samples, then $g^Q(q)$ is, for large systems, twice as wide as spikes are.

D. Equilibration times

We now explain how we make sure that thermal equilibrium is reached before we start taking measurements. To this end, some quantities are next defined. First, a pair of identical replicas of a given sample are allowed to evolve independently in time, starting at $t = 0$ from two uncorrelated random spin configurations. Let q_t be the overlap between the configurations of the two identical replicas at time t. In addition, let $q_2(t)$ be the average of q_t^2 over all samples. During equilibration $q_2(t)$ is expected to increase up to its equilibrium value. Semilog plots of $q_2(t)$ versus t displayed in Fig. 1 for $x = 0.35$, $L = 8, 10$ and the lowest used temperatures show
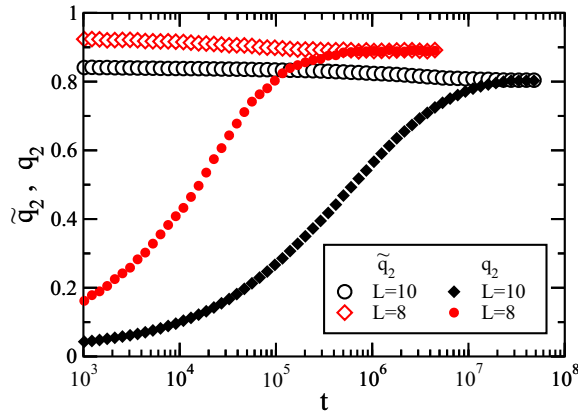
FIG. 1. (Color online) Semilog plots of $\widetilde{q}_2(t_0,t)$ and q_2 vs time t (in MC sweeps) for DIS systems with concentration $x = 0.35$ running at the lowest temperature T_n for the values of L indicated in the figure. $T = 0.075$ ($T = 0.05$) for $L = 10$ ($L = 8$). q_2 is obtained from averages of q^2 over time, starting at $t = 0$ from an initial random spin configuration. Here $t_0 = 5 \times 10^7$ MC sweeps for $L = 10$, and 5×10^6 MCS for $L = 8$. Data points at time t stand for an average over a time interval $[t, 1.2t]$ and over 10^3 samples.

that a stationary value q_2 is reached only after some millions of MC sweeps.

In order to check whether this stationary value q_2 is an equilibrium one, we define a second overlap, $\widetilde{q}_t$, not between configurations of pairs of identical replicas at the same time t, but between spin configurations of a single replica taken at two different times t_0 and $t_1 = t_0 + t$ of the same MC run,

$$\widetilde{q}_t(t_0) = N^{-1} \sum_j \sigma_j(t_0)\sigma_j(t_0 + t). \quad (12)$$

Let $\widetilde{q}_2(t_0, t)$ be the average of $(\widetilde{q}_t(t_0))^2$ over all samples. Suppose thermal equilibrium is reached long before time t_0 has
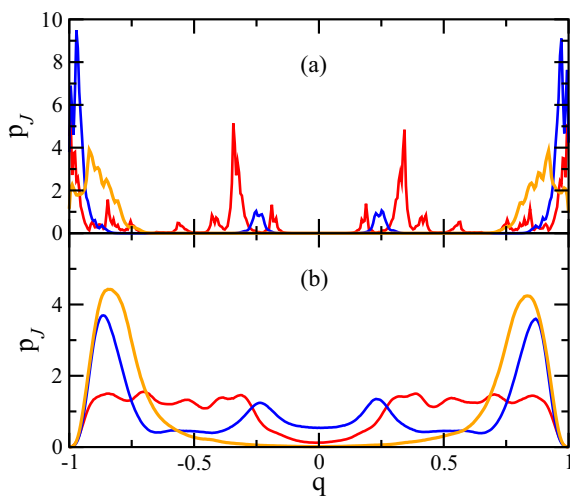

FIG. 2. (Color online) (a) Overlap distributions $p_{\mathcal{J}}(q)$ for DIS systems with $L = 10$, $x = 0.35$ and $T = 0.1$ for three samples with different realizations of disorder. For each sample we collect values of q over 5×10^7 MC sweeps. (b) The same as in (a) but for $T = 0.25$ for the same sample set. Recall that the transition temperature is $T_{sg} = 0.35$.

elapsed. Then $\widetilde{q}_2(t_0,t)$ and $q_2(t)$ should tend towards a common value q_2 as $t \to t_0$. Plots of $\widetilde{q}_2(t_0,t)$ vs t are shown in Fig. 1 for $t_0 = 5 \times 10^7$ MC sweeps (5×10^6 MCS sweeps) for $L = 10$ ($L = 8$) for the same values of x and T as for $q_2(t)$. Note that both quantities, $\widetilde{q}_2(t_0,t)$ and $q_2(t)$, do become approximately equal when $t \to t_0$. In order to obtain equilibrium results, we have always chosen sufficiently large values of t_0 to make sure that $\widetilde{q}_2(t_0,t) \approx q_2(t)$ for $t \gtrsim t_0$. In our simulations, we let each system equilibrate for a time t_0 and take averages over the time interval $[t_0, 2t_0]$. All values of t_0 and N_s are given in Table II.

It has recently been shown that equilibration times increase with the roughness of the free-energy landscape of each individual sample [38]. Numerous spikes in overlap distributions $p_{\mathcal{J}}^Q$ are the signature of samples that have numerous minima in their free-energy landscape. Visual inspection of overlap distributions of samples like the ones shown in Fig. 2 shows fairly symmetric $p_{\mathcal{J}}^Q$ curves even though some of them have several spikes. Then our stringent equilibration criterion suggests that nearly all the samples are well equilibrated.

III. RESULTS

A. Overlap distributions

As it has been found for other SG models, it is interesting to examine individual samples of DIS. In Fig. 2(a) we plot $p_{\mathcal{J}}(q)$ versus q for different samples at temperature $T/T_{sg} \simeq 0.3$. At this low temperature, some $p_{\mathcal{J}}(q)$ display well-defined spikes centered on small q values, which seems to vary randomly from sample to sample. Qualitatively similar distributions have been observed for the EA and SK models [18,19,39]. It is clear that these inner peaks (that is, peaks away from $q \approx \pm 1$) come from overlaps between states that belong to different basins of attraction. The main aim of this paper is to extract statistical information for these *cross-overlap* (CO) spikes situated on the interval $q \in (-Q, Q)$. Similar plots for higher temperatures [see Fig. 2(b) for $T/T_{sg} \simeq 0.7$] show that thermal fluctuations render individual spikes not clearly discernible. Then, in order to explore well within the SG phase, we have chosen the lowest temperature in our TMC simulations to be $0.2T_{sg}$. We report most of our results for $T \leqslant 0.4T_{sg}$. We have also chosen a concentration $x = 0.35$ which is far below the threshold for the AF phase. Both low temperatures and low concentrations result in large equilibrium times t_0. In addition, in order to obtain good sample statistics we need to simulate a large number N_s of samples for all system sizes studied. All of this has restricted us to deal with relatively modest system sizes in our simulations. The simulation parameters are given in Tables I and II.

Figure 3(a) shows the sample-averaged overlap distribution $p(q)$ for DIS at $T = 0.1$. At this low temperature, $p(q)$ exhibits two large peaks at $\pm q_m$ with $q_m \approx 1$ and a relatively flat plateau with $p(0) \neq 0$ in the region $q \in (-Q, Q)$ for, say, $Q \approx 1/2$. The nonzero $p(0)$ value does not change with L for the system sizes studied. This behavior, known for the SK and EA models [7,15], is in contradiction with the droplet picture of SGs, for which $p(0)$ vanishes as $L^{-\theta}$ [13].

Plots of $(\delta p)^2$ versus p are shown for DIS at the same temperature in Fig. 3(b). $\sqrt{(\delta p)^2}$, a measure of deviations of $p_{\mathcal{J}}(q)$ from the average $p(q)$, is clearly greater than p for $q \in (-1/2, 1/2)$, indicating lack of self-averaging. More
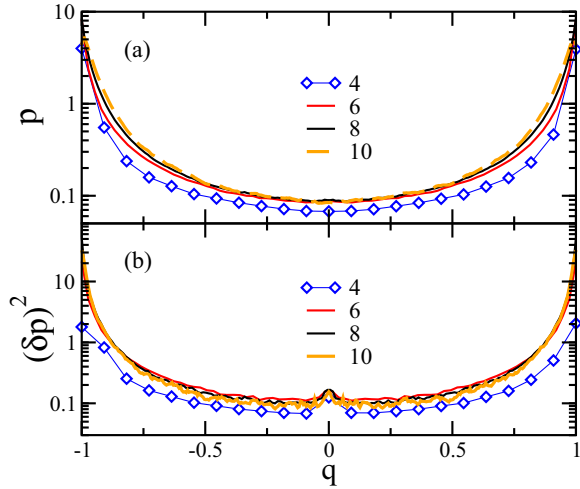
FIG. 3. (Color online) (a) Plots of the averaged distribution $p(q)$ vs q for DIS systems with $x = 0.35$, $T = 0.1$, and the values of L shown. (b) Same as in (a), but for $(\delta p)^2$, the mean-square deviations of $p_{\mathcal{J}}(q)^2$ away from $p(q)$ over all $\mathcal{J}$ samples.

interestingly, $(\delta p)^2$ does not vary appreciably with L. This is at odds with the behavior found in MC simulations for the SK model for which $(\delta p)^2 \propto L$ for $T \leqslant 0.5 T_{sg}$ [33]. Recall that in the RSB scenario, one expects that $p_{\mathcal{J}}(q)$ exhibits with many sharp spikes in the region $q \in (-Q, Q)$ that become δ-like functions as L increases, resulting in a diverging $(\delta p)^2$ for macroscopic systems.

B. Integrated overlap distributions

Here we consider averages of both p and $(\delta p)^2$ over $q \in (-Q, Q)$. This allows us to focus on the contributions of CO spikes and, in addition, to reduce statistical noise if Q is not too small. Plots of X^Q, the sample-averaged area under CO spikes, versus T are shown for $Q = 1/2$ in Figs. 4(a) and 4(b) for DIS and SK models, respectively. In both cases, X^Q is, as far as we can see, size independent at temperatures well
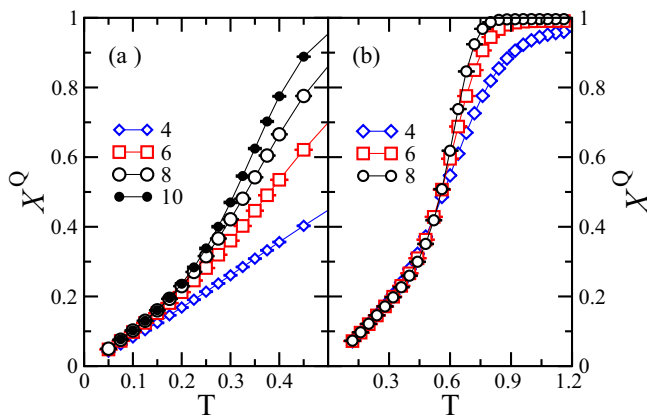

FIG. 4. (Color online) (a) Plot of X^Q versus T for DIS systems with $x = 0.35$, $Q = 1/2$ and the values of L indicated in the figure. (b) The same plots for the SK model, with $Q = 1/2$ and the values of L shown. In both panels, error bars are smaller than symbol sizes.
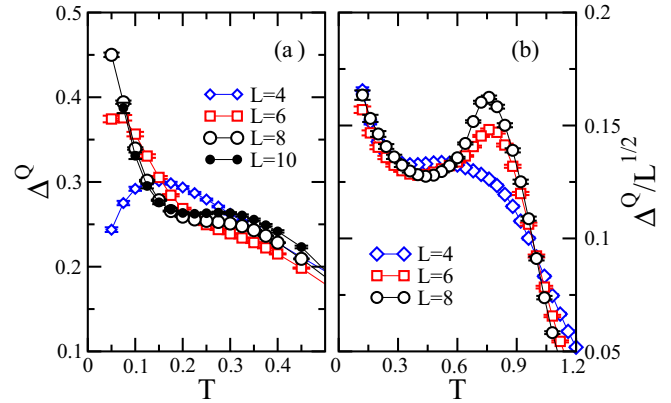

FIG. 5. (Color online) (a) Plot of Δ_Q vs T for DIS systems with $x = 0.35$, $Q = 1/2$ and the values of L indicated in the figure. (b) Plot of $\Delta_Q/L^{1/2}$ versus T for the SK model, with $Q = 1/2$.

below T_{sg}. We obtain quantitatively similar results (not shown) for $Q = 1/4$. This is a strong piece of evidence against the validity of the droplet picture, for which X^Q is expected to vanish as $T L^{-\theta}$ [13]. A similar behavior has been found for the EA model in several MC simulations [15,19]. However, it has been argued that strong finite-size effects may mask the asymptotic behavior at the system sizes currently available to MC simulation [16]. Finally, we note that in Figs. 4(a) and 4(b) X^Q seems to vanish as $T \to 0$ (as was long ago predicted for the SK model) [40].

Plots of Δ^Q versus T for DIS in Fig. 5(a) show the presence of finite-size effects. Note that for small sizes, Δ^Q increases as T decreases only up to $T = 0.15$ ($T = 0.075$) for $L = 4$ ($L = 6$). We return to this point in Sec. III C. More interestingly, curves for larger sizes ($L \geqslant 8$) give a strong indication that Δ^Q does not diverge as L increases. This result is in contradiction with a RSB scenario and is in sharp contrast with the behavior exhibited in Fig. 5(b) for the SK model, for which Δ^Q increases with $\sqrt{L}$ at low temperatures. It is worth mentioning that Δ^Q differs qualitatively from the average $X_2 \equiv [(X_{\mathcal{J}}^Q)^2]_{\mathcal{J}}$ when Q is not very small [19]. X_2 has been investigated in detail in several papers and it is known to be size independent for both the EA and SK models [17].

C. Pair correlation functions

Data points for the pair correlation function g^Q for $Q = 1/2$ are shown in Figs. 6(a) and 6(b) for the SK model at $T = 0.2$ and DIS at $T = 0.075$, respectively. Note that these temperatures are such as $T/T_{sg} \simeq 0.2$ in both cases. We find curves that are rather pointed with widths clearly smaller than Q. We obtain similar results for $Q = 1/4$. Data for DIS in Fig. 6(b) do not exhibit any significant size dependence. In contrast, g^Q curves for SK in Fig. 6(a) become sharper as L increases. This result for the SK model is as expected for a RSB scenario. In the RSB solution, $p_{\mathcal{J}}(q)$ is made of several cross-overlap spikes that for small values of q become δ functions in the macroscopic limit and densely fill the interval $q \in (-Q, Q)$. In striking contrast, our result for DIS suggest that the number of SG states do not grow with L at finite low temperatures.
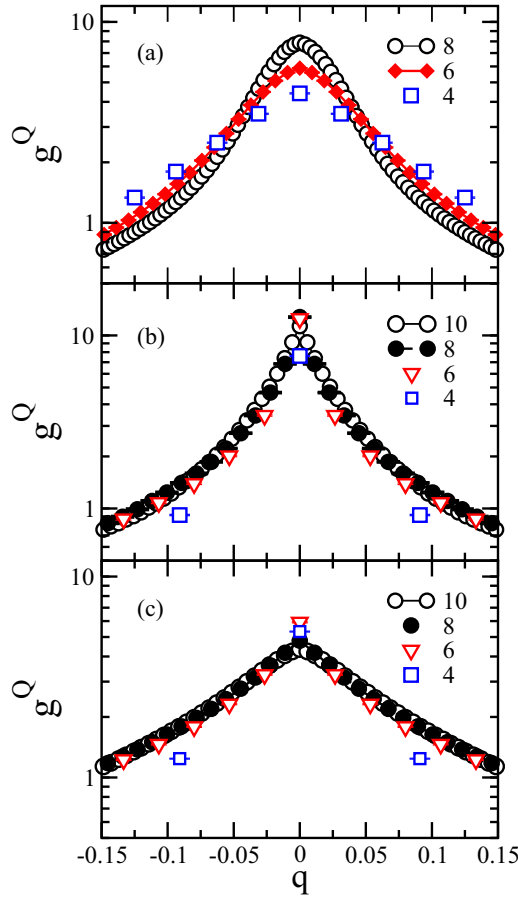
FIG. 6. (Color online) (a) Plots of g^Q vs q for the SK model at $T = 0.2$ with $Q = 1/2$ and the values of L shown. (b) Same plot as for (a) but for DIS systems with $x = 0.35$ at $T = 0.075$. (c) Same plot as for (b) but for $T = 0.125$.

Some people have argued that comparing data for different models (EA and SK) at the same value of T/T_{sg} is not meaningful. They find it more appropriate to make such a comparison at temperatures for which X^Q values are the same [21]. We follow this recipe and compare the data shown in Fig. 6(c) for DIS at $T = 0.125$ and in Fig. 6(a) for the SK model at $T = 0.2$. Apart from the fact that g^Q becomes narrower as T decreases, we do not notice any qualitative difference.

It is interesting to note that spikes, even though they have nonzero widths w at finite T, may not be discerned in $p_{\mathcal{J}}(q)$ distributions of very small systems. Note that the minimum appreciable value of q for systems of N spins is given by $\Delta q = 2/N$. Thus, finite-size effects are expected to come at very low T when $w \lesssim \Delta q$. This seems to be the case for the data shown in Figs. 5(a) and 7(a) for $L = 4$ ($L = 6$) and $T \lesssim 0.15$ ($T \lesssim 0.075$).

Plots of w^Q versus T are shown in Figs. 7(a) and 7(b) for DIS and the SK model, respectively. w^Q appear in Fig. 7(a) to be size independent at least for $L \geqslant 8$. This points to finite widths for CO spikes in the $L \to \infty$ limit for low (but finite) temperature. On the other hand, w^Q values for the SK model displayed in Fig. 7(b) appear to vanish as $1/L^{1/2}$ as L increases at least for $T \lesssim 0.4$, in agreement with the RSB picture.
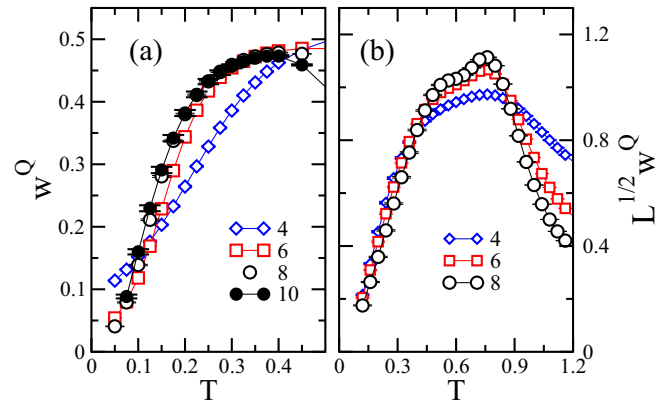

FIG. 7. (Color online) (a) Plots of wQ vs q for DIS systems with $x = 0.35$ for $Q = 1/2$ and the values of L shown. (b) Plots of $L^{1/2}wQ$ vs q for (a) but for the SK model, $Q = 1/2$ and the values of L shown. In both panels all error bars are smaller than symbol sizes.

D. Cumulative distributions

As interesting as they could be, pair correlation functions (PCFs) do only give information on how spiky sample distributions $p_{\mathcal{J}}(q)$ are in the $(-Q, Q)$ region. However, PCFs do not give any information about the height of spikes located there. Following seminal work by Yucesoy *et al.* [18], we study here $\Pi_c^{\widetilde{p}}(z)$, the fraction of samples without any spike in $(-Q, Q)$ with height larger than z. Plots of $\Pi_c^{\widetilde{p}}$ versus z for DIS at $T = 0.1$ are shown in Fig. 8(a). They give a strong indication that $\Pi_c^{\widetilde{p}}$ reach a size-independent shape for $L \geqslant 8$ for a wide range of values of z. In order to check for the robustness of our $\Pi_c^{\widetilde{p}}(z)$ values, we have grouped all available samples in K ensembles of 10^3 samples each, calculated $\Pi_c^{\widetilde{p}}$ for each ensemble $k = 1, \ldots, K$, and obtained the standard deviation (SD) of the K resulting values. Tiny vertical bars in Figs. 8 and 9 stand for such SDs. Plots in Fig. 8(a) are to be compared with the ones displayed in Fig. 8(b) for the SK model. Note in
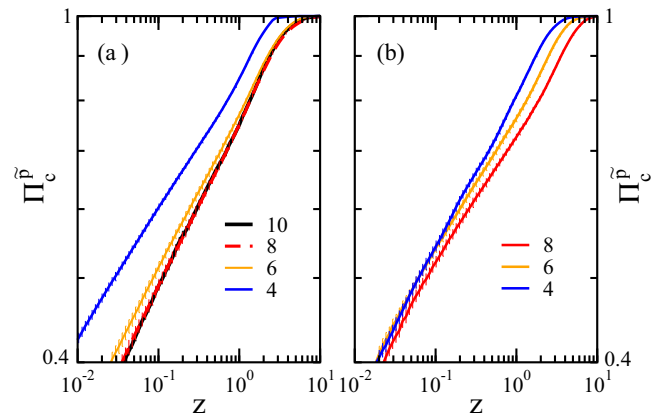

FIG. 8. (Color online) (a) Plot of the cumulative distribution $\Pi\{\widetilde{p}_{\mathcal{J}}^Q\}$ versus x for DIS systems with $x = 0.35$, for $Q = 1/2$, $T = 0.1$ and the values of L indicated in the figure, where $\widetilde{p}_{\mathcal{J}}^Q$ is the maximum value of $p_{\mathcal{J}}(q)$ over the interval $-Q \leqslant q \leqslant Q$. (b) The same plot as in (a) but for the SK model, for $Q = 1/2$, $T = 0.16$ and the values of L shown.
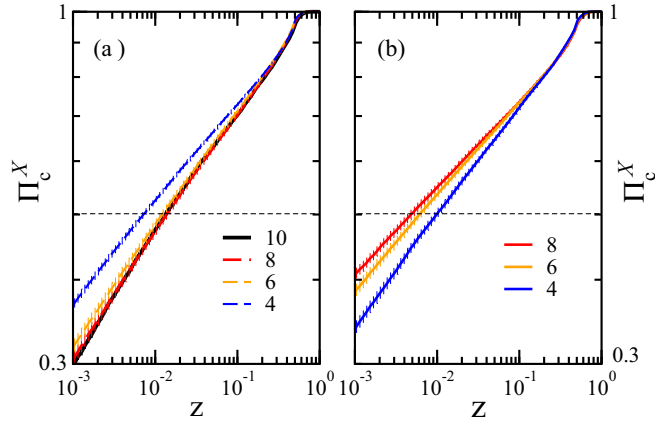
FIG. 9. (Color online) (a) Plot of the cumulative distribution $\Pi\{X_{\mathcal{J}}^{Q}\}$ versus x for DIS systems with $x = 0.35$ for $T = 0.1$ and the values of L indicated in the figure. (b) The same plots as in (a) but for the SK model for $T = 0.16$.

Fig. 8(b) that, at least for $z \gtrsim 0.5$, $\Pi_c^{\tilde{p}}(z)$ clearly decreases as L increases, indicating a proliferation of high spikes for larger sizes. This is as expected for the RSB picture, for which CO spikes become δ-like functions in the thermodynamic limit.

Finally, we report results on how the random variable $X_{\mathcal{J}}^{Q}$ is distributed. Previous MC simulations have found a similar behavior for the EA and SK models when dealing with the cumulative distribution $\Pi_c^X(z)$ of quantity $z = X_{\mathcal{J}}^{Q}$ [18,20]. The mean-field theory of the SK model offers precise predictions on $\Pi_c^X(z)$ and their moments [17]. In particular, $\Pi_c^X(z)$ is found to follow a power law for small z. For small values of Q [41], $\Pi_c^X(z) \propto z^y$, where y stands here for X^Q. Some people have found it useful to study the *median* of the cumulative distribution, which is predicted to reach a nonzero value in the thermodynamic limit in the RSB picture but vanishes for the droplet model. Log-log plots of Π_c^X versus X for DIS displayed in Fig. 9(a) show curves with power-law behavior for small z. Data do not show any significant deviation for sizes $L \geqslant 8$. The *median* (marked by the crossings points of the curves with the horizontal dotted line in the figure) decreases as L increases reaching a nonzero value. The counterpart plots for the SK model are shown in Fig. 9(b). In agreement with previous MC work on the SK model [20,23], we find strong finite-size effects. However, curves seem to converge to some limiting curve as L increases [20]. Note that, in contrast with DIS, the *median* of Π_c^X increases as L increases. All our results for Π_c^X for both the SK model and DIS are not in contradiction with a RSB scenario.

IV. CONCLUSIONS AND DISCUSSION

By tempered Monte Carlo calculations, we have studied the low-temperature behavior of a diluted system of classical dipoles placed on a SC lattice. These dipoles are Ising spins randomly placed on a fraction x of all lattice sites and point up or down along a common crystalline axis.

Previous MC studies [19] for this model have provided strong evidence for the existence of a SG phase for $x \lesssim 0.65$ with a SG transition temperature $T_{\text{sg}}(x) \simeq x$. The SG phase was then found to have quasi-long-range order, as in the 2D-XY model [42]. Neither the droplet model nor a RSB scenario fit with this marginal behavior. Despite the existence of this *soft* SG order, we find in our simulations spiky overlap distributions $p_{\mathcal{J}}(q)$ that are strongly sample dependent, as previously found in simulations for the EA and the SK models [18,19,39].

We have studied the statistics of $p_{\mathcal{J}}(q)$ for $q \in (-Q, Q)$ using some recently proposed observables [18–20]. We find that $p(q)$ and $\delta p(q)$ (as well as their integrated counterparts X^Q and Δ^Q) do not vary appreciably with L.

From a suitable defined pair correlation function [19] we compute an averaged width w^Q that appears to remain finite as L increases. Complementary to this result, we find that the fraction of samples with spikes higher than a certain threshold does not vary appreciably with L. All of this points to finite width for CO spikes in the $L \to \infty$ limit at low temperatures.

Our results are in clear contradiction with droplet model predictions. On the other hand, a direct comparison of our data with MC data obtained for the SK model shows that crucial RSB predictions are also at odds with some of our results. It is noteworthy that the findings enumerated above for DIS are strikingly similar to the ones found in previous MC work for the EA model [18–20,23], though finite-size effects have been reported to be strong for the EA model for the available systems sizes in MC simulations.

[1] S. E. Page, *Diversity and Complexity* (Princeton University Press, Princeton, NJ, 2010); S. Lloyd, IEEE Control Syst. Mag. **21**, 7 (2001); R. N. Mantegna and H. E. Stanley, *An Introduction to Econophysics: Correlations and Complexity in Finance* (Cambridge University Press, Cambridge, UK, 2000).

[2] G. Parisi, arXiv:cond-mat/9412018v1 (1994); T. Aspelmeier, A. J. Bray, and M. A. Moore, Phys. Rev. Lett. **92**, 087203 (2004).

[3] D. Sherrington and S. Kirkpatrick, Phys. Rev. Lett. **35**, 1792 (1975); S. Kirkpatrick and D. Sherrington, Phys. Rev. B **17**, 4384 (1978).

[4] G. Toulouse, Commun. Phys. **2**, 115 (1997).

[5] D. L. Stein and C. M. Newman, *Spin Glasses and Complexity* (Princeton University Press, Princeton, NJ, 2012).

[6] M. Mézard, G. Parisi, and M. Virasoro, *Spin Glass Theory and Beyond* (World Scientific, Singapore, 2004).

[7] J. Thouless, P. W. Anderson, and R. Palmer, Philos. Mag. **35**, 593 (1977); A. J. Bray and M. A. Moore, Phys. Rev. Lett. **41**, 1068 (1978).

[8] G. Parisi, Phys. Rev. Lett. **43**, 1754 (1979); **50**, 1946 (1983); for a review, see E. Marinari, G. Parisi, and J. J. Ruiz-Lorenzo, in *Spin Glasses*, edited by K. H. Fischer and J. A. Hertz, (Cambridge University Press, Cambridge, 1991); E. Marinari, G. Parisi, F. Ricci-Tersenghi, J. J. Ruiz-Lorenzo, and F. Zuliani, J. Stat. Phys. **98**, 973 (2000).

[9] K. Binder and A. P. Young, Rev. Mod. Phys. **58**, 801 (1986).

[10] S. F. Edwards and P. W. Anderson, J. Phys. F **5**, 965 (1975).

[11] R. N. Bhatt and A. P. Young, Phys. Rev. Lett. **54**, 924 (1985); A. T. Ogielski and I. Morgenstern, *ibid.* **54**, 928 (1985); R. N. Bhatt and A. P. Young, Phys. Rev. B **37**, 5606 (1988).

[12] C. M. Newman and D. L. Stein, Phys. Rev. E **57**, 1356 (1998); Phys. Rev. Lett. **76**, 4821 (1996).

[13] D. S. Fisher and D. A. Huse, J. Phys. A **20**, L1005 (1987); Phys. Rev. B **38**, 386 (1988); M. A. Moore, H. Bokil, and B. Drossel, Phys. Rev. Lett. **81**, 4252 (1998); M. A. Moore, J. Phys. A **38**, L783 (2006).

[14] F. Krzakala and O. C. Martin, Phys. Rev. Lett. **85**, 3013 (2000); M. Palassini and A. P. Young, *ibid.* **85**, 3017 (2000).

[15] H. G. Katzgraber, M. Palassini, and A. P. Young, Phys. Rev. B **63**, 184422 (2001).

[16] A. A. Middleton, Phys. Rev. B **87**, 220201 (2013).

[17] R. A. Baños, A. Cruz, L. A. Fernandez, J. M. Gil-Narvion, A. Gordillo-Guerrero, M. Guidetti, D. Iñiguez, A. Maiorano, F. Mantovani, E. Marinari, V. Martin-Mayor, J. Monforte-Garcia, A. Muñoz Sudupe, D. Navarro, G. Parisi, S. Perez-Gaviro, F. Ricci-Tersenghi, J. J. Ruiz-Lorenzo, S. F. Schifano, B. Seoane, A. Tarancón, R. Tripiccione, and D. Yllanes, Phys. Rev. B **84**, 174209 (2011).

[18] B. Yucesoy, H. G. Katzgraber, and J. Machta, Phys. Rev. Lett. **109**, 177204 (2012).

[19] J. F. Fernández and J. J. Alonso, Phys. Rev. B **86**, 140402(R) (2012); **87**, 134205 (2013).

[20] A. Billoire, A. Maiorano, E. Marinari, V. Martin-Mayor, and D. Yllanes, Phys. Rev. B **90**, 094201 (2014).

[21] A. Billoire, L. A. Fernandez, A. Maiorano, E. Marinari, V. Martin-Mayor, G. Parisi, F. Ricci-Tersenghi, J. J. Ruiz-Lorenzo, and D. Yllanes, Phys. Rev. Lett. **110**, 219701 (2013).

[22] Creighton K. Thomas, David A. Huse, and A. A. Middleton, Phys. Rev. Lett. **107**, 047203 (2011).

[23] M. Wittmann, B. Yucesoy, H. G. Katzgraber, and J. Machta, and A. P. Young, Phys. Rev. B **90**, 134419 (2014).

[24] C. Wengel, C. L. Henley, and A. Zippelius, Phys. Rev. B **53**, 6543 (1996).

[25] J. Luttinger and L. Tisza, Phys. Rev. **72**, 257 (1947).

[26] J. F. Fernández and J. J. Alonso, Phys. Rev. B **62**, 53 (2000).

[27] W. Luo, S. R. Nagel, T. F. Rosenbaum, and R. E. Rosensweig, Phys. Rev. Lett. **67**, 2721 (1991).

[28] A. H. Cooke, D. A. Jones, J. F. A. Silva, and M. R. Wells, J. Phys. C: Solid State Phys. **8**, 4083 (1975).

[29] J. Villain, Z. Physik B **33**, 31 (1979).

[30] D. H. Reich, B. Ellman, J. Yang, T. F. Rosenbaum, G. Aeppli, and D. P. Belanger, Phys. Rev. B **42**, 4631 (1990); W. Wu, D. Bitko, T. F. Rosenbaum, and G. Aeppli, Phys. Rev. Lett. **71**, 1919 (1993); C. Ancona-Torres, D. M. Silevitch, G. Aeppli, and T. F. Rosenbaum, *ibid.* **101**, 057201 (2008).

[31] K. M. Tam and M. J. P. Gingras, Phys. Rev. Lett. **103**, 087202 (2009).

[32] J. C. Andresen, H. G. Katzgraber, V. Oganesyan, and M. Schechter, Phys. Rev. X **4**, 041016 (2014).

[33] J. J. Alonso and J. F. Fernández, Phys. Rev. B **81**, 064408 (2010).

[34] M. Palassini and S. Caracciolo, Phys. Rev. Lett. **82**, 5128 (1999).

[35] E. Marinari and G. Parisi, Europhys. Lett. **19**, 451 (1992); K. Hukushima and K. Nemoto, J. Phys. Soc. Jpn. **65**, 1604 (1996).

[36] J. F. Fernández, Phys. Rev. B **78**, 064404 (2008); J. F. Fernández and J. J. Alonso, *ibid.* **79**, 214424 (2009).

[37] N. A. Metropolis, A. W. Rosenbluth, M. N. Rosenbluth, A. H. Teller, and E. Teller, J. Chem. Phys. **21**, 1087 (1953).

[38] B. Yucesoy, J. Machta, and H. G. Katzgraber, Phys. Rev. E **87**, 012104 (2013).

[39] T. Aspelmeier, A. Billoire, E. Marinari, and M. A. Moore, J. Phys. A **41**, 324008 (2008).

[40] J. Vannimenus, G. Toulouse, and G. Parisi, J. Phys. (Paris) **42**, 565 (1981).

[41] M. Mézard, G. Parisi, N. Sourlas, G. Toulouse, and M. Virasoro, Phys. Rev. Lett. **52**, 1156 (1984).

[42] J. M. Kosterlitz and D. J. Thouless, J. Phys. C **6**, 1181 (1973); J. M. Kosterlitz, *ibid.* **7**, 1046 (1974); see also, J. V. José, L. P. Kadanoff, S. Kirkpatrick, and D. R. Nelson, Phys. Rev. B **16**, 1217 (1977); J. Villain, J. Phys. (Paris) **36**, 581 (1975); J. F. Fernández, M. F. Ferreira, and J. Stankiewicz, Phys. Rev. B **34**, 292 (1986); H. G. Evertz and D. P. Landau, *ibid.* **54**, 12302 (1996).